Supplementary information

I. EXPERIMENT

The Ce:YAG samples' Ce concentrations are 0.08%. They are produced by Shanghai Changjing Optoelectronics Co., Ltd, and their sizes are 5mm $\times$ 5mm $\times$ 0.5mm.

The experiment is divided into two parts: the writing part and the reading part. The writing experiment is performed on a home-built laser-writing setup as shown in Fig. S1(a). We used a 450nm laser (Changchun New Industries Optoelectronics Technology MLL-III-450L-80mW) switched on and off by an acousto-optic modulator (AOM). An attenuator (Thorlabs ZX73-2500-S+) regulating AOM's input waveform controls the laser power. A 4-f system was constructed with a two-axis Galvo scanner (Coremorrow P35A.T40S) and two f=200 mm concave mirrors (Thorlabs CM508-200-P01) to form the scanning system. An air objective lens (Newport M-10x, 0.25 N.A.) was used to focus the beam. The sample is placed vertically on a linear stage (Newport M-562-XYZ) to locate the relative writing position on crystals and focus manually . The reading experiment is achieved in a dark room, and the apparatus is shown in Fig. S1(b). The sample is placed on a hot plate (Heidolph) and heated to 275°C. The fluorescence image is magnified by optical microscopy (Gaopin GP-560H) and captured by a monochrome CMOS camera (Thorlabs CS165MU/M).

The experiment process is illustrated in Fig. S2. We prepared an empty crystal (Fig. S2(a)) and placed it in the laser writing setup to record the image (Fig. S2(b)). The image is 1000px $\times$ 1000px. 1px in the image corresponds to 1.12μm on the crystal in our setup. The laser's power is 100μw, 200μw, 400μw, etc., corresponding to its grayscale layer. Each pixel is exposed for 1 ms. The written crystal has no visible difference compared with the

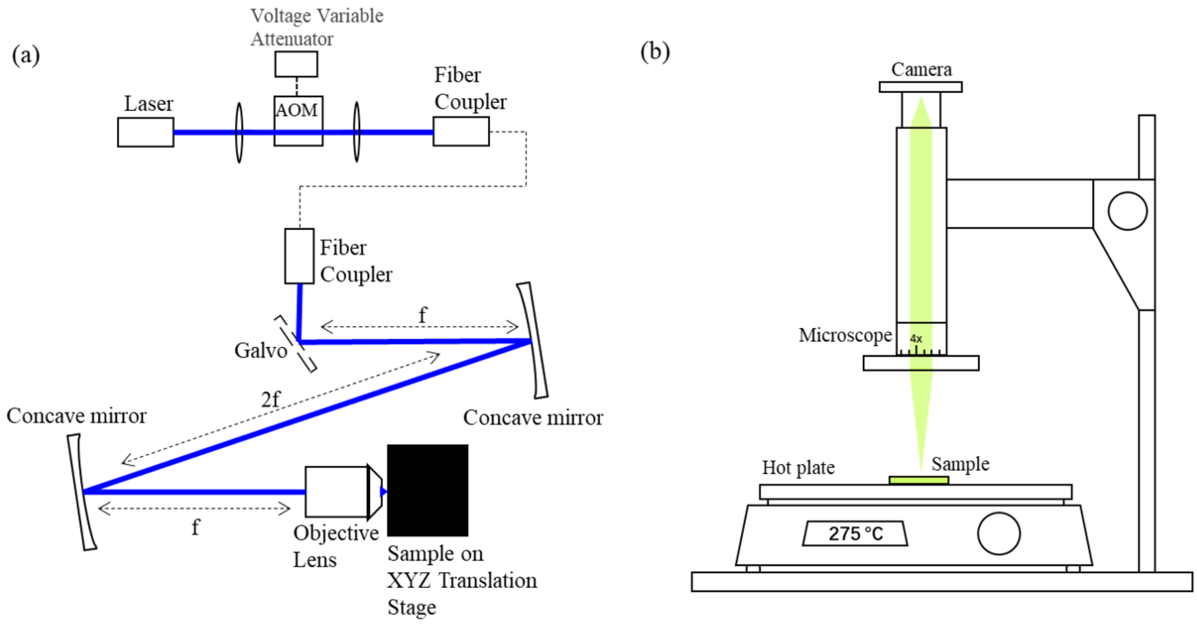

FIG. S1: Experiment apparatus. (a) The laser writing setup. (b) The readout apparatus.

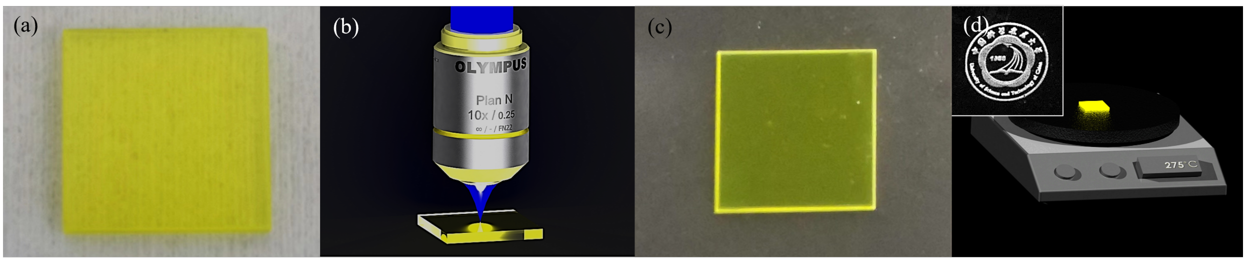

FIG. S2: Experiment process. (a) Cleaned Ce:YAG crystals. (b) Optical information storage via laser writing. (c) Information stored crystals. No visible difference compared to (a). (d) Information readout on the hotplate. The inset picture is a stored and TL readout logo of University of Science and Technology of China.

empty crystal (Fig. S2(c)). When the image needs to be read out, we heat the written crystal on a hotplate (Fig. S2(d)). The image will be captured by the camera, with 250ms exposure time and 30dB gain. The video is shown in Fig. S3, and each frame is presented in Fig. S3(a). As shown in the fluorescence brightness diagram in Fig. S3(b), the information is wiped out in the last frame. We finally add all frames to obtain the final image in Fig. S3(c).

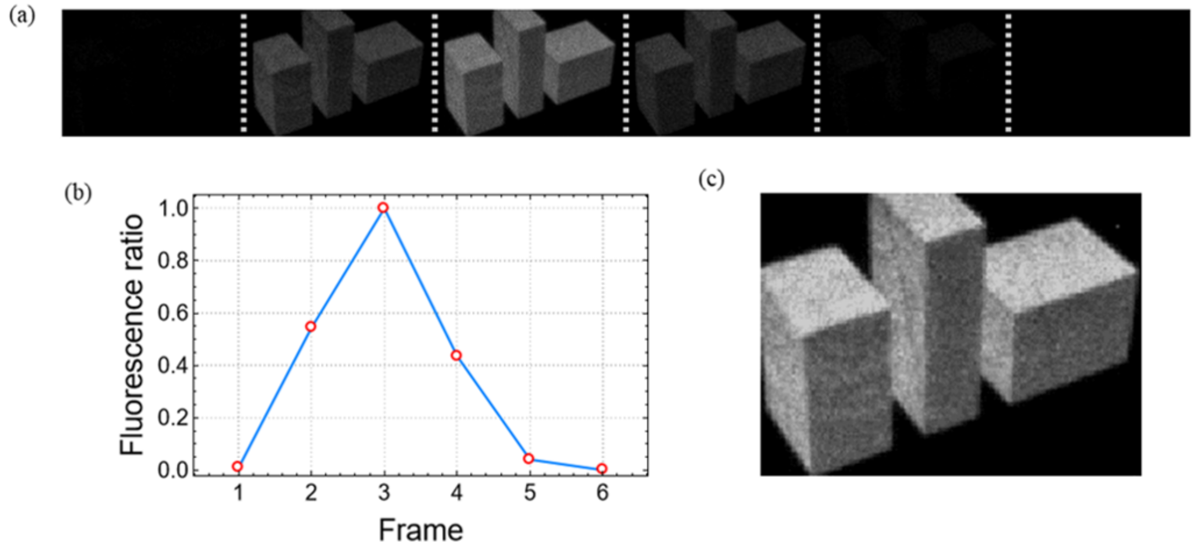

FIG. S3: Demonstration of readout. (a) The captured video's frames. The information is wiped out after reading. (b) The normalized average fluorescence brightness of each frame. (c) Add all frames to obtain the final image.

II. ALGORITHM OF IMAGE SHARPENING

The facula diffusion would cause inaccuracy and blurriness in the readout image. The edge of a grayscale layer is blurry, and layers cannot be accurately discriminated in post-process. Worse still, the gray values in the junction between a low-gray-value layer and a high-gray-value layer are middle-gray-value. They will intrude into the actual middle-gray-value layer, leaving disturbing lines in the middle layer during post-process. Therefore, an image sharpening algorithm is needed.

Around the junction of two neighboring grayscale layers, pixels' gray values are between the two layers and should be reassigned to any of them. We propose a simple algorithm to accomplish this task. Firstly, we perform Gaussian blurring with a radius of r_1 to increase the SNR. Afterward, in each pixel, we calculate the maximal and minimal gray value in the surrounding pixels within a radius of r_2, and reassign the pixel's gray value to the closer one

FIG. S4: Demonstration of the algorithm. (a) The raw picture captured. The junction between two gray layers is blurry, and the SNR is relatively low. (b) Blur the raw picture. The SNR is highly increased. (c) Apply the sharpening algorithm to the blurred picture. The junction is processed to be sharp and clear.

between the maximal gray value and minimal gray value in the surrounding.

A demonstration is presented in Fig. S4. The raw picture is shown in Fig. S4(a). Its SNR is so low that any sharpening algorithm could lead to a disastrous result. Therefore, we blur the image to increase SNR, as shown in Fig. S4(b). Subsequently, we can apply our sharpening algorithm. We can get an image with sharp edge by tuning r_1 and r_2. The simple algorithm effectively sharpens the image as shown in Fig. S4(c). It should be noted that the algorithm is rather simple that it only serves for the principal demonstration of multi-gray-value storage methods, and there should be more powerful algorithms to be developed.

III. POST-PROCESS

After we capture the raw image, we inspect the histogram of its gray value, as shown in Fig. S5(a). It should be noted that the image does not have the 7th layer, and the 0th layer is the black background. We can identify 7 peaks corresponding to 7 layers. However, the gray values between layers aren't 0. They will leave annoying lines in the separated pictures. Therefore, we apply the algorithm described above, and the result is shown in Fig. S5(b). The histogram shows great improvement in sharper peaks and lower values between

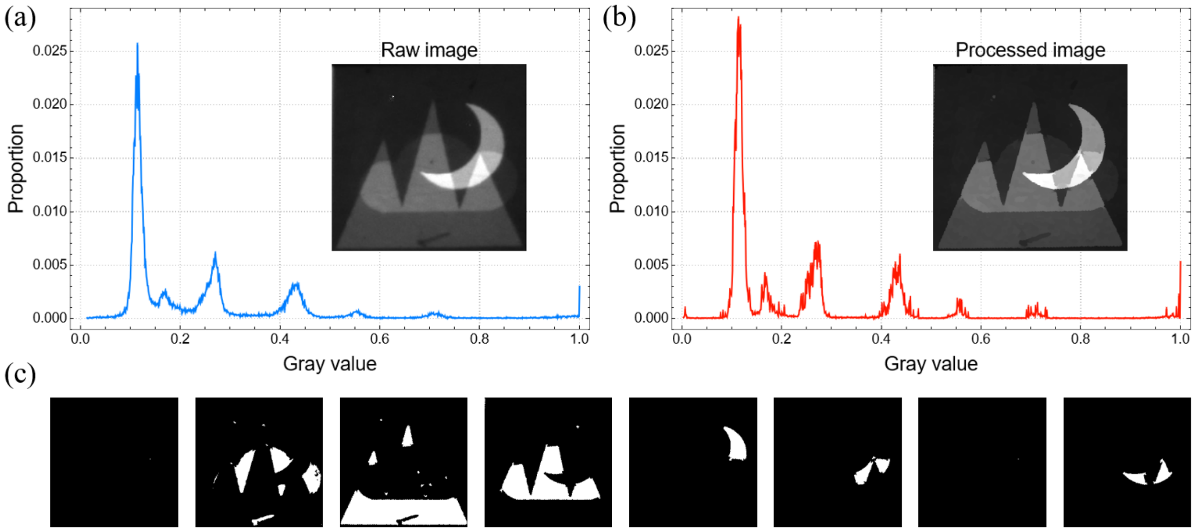

FIG. S5: Post-process (a) Raw image and histogram of its gray values. There are 7 peaks. The non-zero values between peaks will badly affect the separation result. (b) Processed image and histogram of its gray values. The peaks are sharper and the values between peaks are lower. (c) The separated layers of the processed image.

peaks, which enables us to cleanly separate each layer, as shown in Fig. S5(c). They can be recombined to retrieve the original pictures, as shown in Fig. 4.